

NON-STURMIAN SEQUENCES OF MATRICES PROVIDING THE MAXIMUM GROWTH RATE OF MATRIX PRODUCTS

VICTOR KOZYAKIN

ABSTRACT. In the theory of linear switching systems with discrete time, as in other areas of mathematics, the problem of studying the growth rate of the norms of all possible matrix products $A_{\sigma_n} \cdots A_{\sigma_0}$ with factors from a set of matrices \mathcal{A} arises. So far, only for a relatively small number of classes of matrices \mathcal{A} has it been possible to accurately describe the sequences of matrices that guarantee the maximum rate of increase of the corresponding norms. Moreover, in almost all cases studied theoretically, the index sequences $\{\sigma_n\}$ of matrices maximizing the norms of the corresponding matrix products have been shown to be periodic or so-called Sturmian, which entails a whole set of “good” properties of the sequences $\{A_{\sigma_n}\}$, in particular the existence of a limiting frequency of occurrence of each matrix factor $A_i \in \mathcal{A}$ in them. In the paper it is shown that this is not always the case: a class of matrices is defined consisting of two 2×2 matrices, similar to rotations in the plane, in which the sequence $\{A_{\sigma_n}\}$ maximizing the growth rate of the norms $\|A_{\sigma_n} \cdots A_{\sigma_0}\|$ is not Sturmian. All considerations are based on numerical modeling and cannot be considered mathematically rigorous in this part; rather, they should be interpreted as a set of questions for further comprehensive theoretical analysis.

1. INTRODUCTION

Various problems of mathematics reduce to the problem of computing the maximum growth rate of the norms of matrix products $A_{\sigma_n} \cdots A_{\sigma_0}$ with factors from a set of matrices \mathcal{A} .

One of the basic, though greatly simplified, examples of this type of situation is found in systems and control theory (Blondel and Canterini, 2003; Blondel and Tsitsiklis, 2000; Brayton and Tong, 1979; Jungers, 2009; Shorten et al., 2007; Wu and He, 2020) when considering the asymptotic behavior of solutions of the so-called linear switching system with discrete time, whose dynamics is described by the equation

$$x_{n+1} = A_{\sigma_n} x_n, \quad \sigma_n \in \{0, 1, \dots, m-1\}, \quad n \geq 0, \quad (1)$$

where $A_{\sigma_i} \in \mathcal{A} := \{A_0, A_1, \dots, A_{m-1}\}$. The solutions for system (1) may be represented as follows:

$$x_n = A_{\sigma_{n-1}} \cdots A_{\sigma_1} A_{\sigma_0} x_0. \quad (2)$$

Therefore, in studying the question of their asymptotic behavior, we naturally come to the problem of estimating (and preferably computing exactly) the growth rate of the norms $\|A_{\sigma_n} \cdots A_{\sigma_1} A_{\sigma_0}\|$ with arbitrary factors $A_{\sigma_i} \in \mathcal{A}$. Of course, the set of questions related to the analysis of the asymptotic behavior of x_n elements can be extended, but in this paper we will not deal with such generalizations.

It is worth noting that the problem of computing the maximum possible growth rate of the norms of matrix products with factors from a set of matrices is quite general; in particular, numerous problems in other areas of science are reduced to it, for example, in coding theory (Blondel et al., 2006; Moision et al., 2001), computational mathematics (Daubechies and Lagarias, 1992, 2001; Heil and Strang, 1995; Jungers et al., 2008; Maesumi, 1998), and the theory of parallel and distributed computation (Bertsekas and Tsitsiklis, 1989; Chazan and Miranker, 1969).

Currently, the range of questions related to the analysis of the growth rate of the norms of matrix products $A_{\sigma_n} \cdots A_{\sigma_1} A_{\sigma_0}$ is usually considered in the framework of the so-called theory of joint/generalized spectral radius, which emerged in the 1960s (Daubechies and Lagarias, 1992,

2020 *Mathematics Subject Classification.* 93-05, 15A18, 15A60, 65F15.

Key words and phrases. Linear switching systems, infinite matrix products, growth rate, Barabanov norm, Sturmian sequences, Python program.

2001; Lagarias and Wang, 1995; Rota and Strang, 1960) and now has several hundred publications (Kozyakin, 2013a). Moreover, in almost all cases studied theoretically, the index sequences $\{\sigma_n\}$ of matrices maximizing the norms of the corresponding matrix products turned out to be periodic or so-called Sturmian. Both the periodicity and the fact that the index sequences $\{\sigma_n\}$ are Sturmian entail a whole set of “good” properties of the sequences $\{A_{\sigma_n}\}$, in particular the existence of a limiting frequency of occurrence of each matrix factor $A_i \in \mathcal{A}$ (Blondel et al., 2003; Bousch and Mairesse, 2002; Kozyakin, 2005a, 2007).

This may give the false impression that periodic or Sturmian sequences occur every time one tries to maximize the norms of matrix products (at least in the case of a pair of 2×2 matrices). This impression is reinforced by the fact that we are not aware of any theoretical studies in this area, apart from those leading to the appearance of periodic or Sturmian sequences, which can be explained by the extreme theoretical and technical complexity of the corresponding analysis. The aim of this paper is to refute this impression. To this end, we determine a class of 2×2 matrices consisting of two matrices similar to rotations of the plane in which the sequence $\{A_{\sigma_n}\}$ maximizing the growth rate of the norms $\|A_{\sigma_n} \cdots A_{\sigma_0}\|$ is not Sturmian.

Let us describe the structure of the work. The introduction provides a rationale for the topics covered here. Section 2 briefly recalls the main facts and constructions from the theory of joint/generalized spectral radius, among which Barabanov’s Theorem plays a crucial role. Section 3 recalls the concept of extremal trajectories, i.e., trajectories with the maximum rate of increase in a certain Barabanov norm. Here we describe a general approach which, in the case of a pair of 2×2 matrices, reduces the problem of constructing extremal trajectories to the problem of studying iterations of a certain mapping of an interval into itself (or, equivalently, of a circle into itself) with a fairly simple structure. Section 4 recalls the well-known theoretical results on the construction and growth of extremal trajectories, which refer to the case of a pair of nonnegative 2×2 matrices of a special form. This case underlies most modern studies of “nontrivial” situations in joint/generalized spectral radius theory. The above theoretical results are illustrated by examples of computer simulations. Section 5 considers the case of a pair of matrices, each of which is similar to a rotation matrix. Using the results of numerical simulations, it is shown that for such matrices a previously unobserved phenomenon occurs in which the index sequences of the extremal trajectories turn out to be non-Sturmian (Main Claim). For a description of the methods and means for numerical modeling of the behavior of matrix products used in this work, see Section 6.

2. THEORETICAL BACKGROUND

Recall the basic concepts and results related to the theory of joint/generalized spectral radius, following (Kozyakin, 2005a,b, 2007).

Let $\mathcal{A} = \{A_0, \dots, A_{m-1}\}$ be a set of m real $d \times d$ matrices, and $\|\cdot\|$ be some norm in \mathbb{R}^d . For every $n \geq 1$, with every finite sequence $\sigma = \{\sigma_0, \sigma_1, \dots, \sigma_{n-1}\} \in \{0, \dots, m-1\}^n$ we link the matrix

$$A_\sigma = A_{\sigma_{n-1}} \cdots A_{\sigma_1} A_{\sigma_0},$$

and define two numerical values:

$$\rho_n(\mathcal{A}) = \max_{\sigma \in \{0, \dots, m-1\}^n} \|A_\sigma\|^{1/n}, \quad \bar{\rho}_n(\mathcal{A}) = \max_{\sigma \in \{0, \dots, m-1\}^n} \rho(A_\sigma)^{1/n},$$

where $\rho(\cdot)$ denotes the spectral radius of a matrix. In these designations, the limit

$$\rho(\mathcal{A}) = \limsup_{n \rightarrow \infty} \rho_n(\mathcal{A}),$$

which does not depend on the choice of the norm $\|\cdot\|$ (and in fact coincides with the limit $\rho(\mathcal{A}) = \lim_{n \rightarrow \infty} \rho_n(\mathcal{A})$) is called the *joint spectral radius* of the set of matrices \mathcal{A} (Rota and Strang, 1960). Similarly, we can consider the limit

$$\bar{\rho}(\mathcal{A}) = \limsup_{n \rightarrow \infty} \bar{\rho}_n(\mathcal{A}),$$

called the *generalized spectral radius* of the matrix set \mathcal{A} (Daubechies and Lagarias, 1992). The values $\rho(\mathcal{A})$ and $\bar{\rho}(\mathcal{A})$ for bounded families of matrices \mathcal{A} actually coincide with each other (Berger and Wang, 1992), and, moreover, for any n , the following inequalities hold:

$$\bar{\rho}_n(\mathcal{A}) \leq \bar{\rho}(\mathcal{A}) = \rho(\mathcal{A}) \leq \rho_n(\mathcal{A}). \quad (3)$$

It follows from the definition of the joint spectral radius that for each $\varepsilon > 0$ the rate of growth of the norms $\|A_\sigma\| = \|A_{\sigma_{n-1}} \cdots A_{\sigma_1} A_{\sigma_0}\|$ for large n does not exceed $(\rho(\mathcal{A}) + \varepsilon)^n$, that is,

$$\|A_\sigma\| = \|A_{\sigma_{n-1}} \cdots A_{\sigma_1} A_{\sigma_0}\| \leq (\rho(\mathcal{A}) + \varepsilon)^n \quad (4)$$

for each finite sequence of indices

$$\sigma = \{\sigma_0, \sigma_1, \dots, \sigma_{n-1}\} \in \{0, \dots, m-1\}^n.$$

Moreover, there are arbitrarily large n and sequences of indices σ for which¹

$$\rho(A_\sigma) = \rho(A_{\sigma_{n-1}} \cdots A_{\sigma_1} A_{\sigma_0}) \geq (\bar{\rho}(\mathcal{A}) - \varepsilon)^n,$$

and therefore, for such n , by virtue of (3), the inequalities

$$\begin{aligned} \|A_\sigma\| &= \|A_{\sigma_{n-1}} \cdots A_{\sigma_1} A_{\sigma_0}\| \geq \\ &\geq \rho(A_{\sigma_{n-1}} \cdots A_{\sigma_1} A_{\sigma_0}) \geq (\bar{\rho}(\mathcal{A}) - \varepsilon)^n \equiv (\rho(\mathcal{A}) - \varepsilon)^n \end{aligned} \quad (5)$$

will hold.

Inequalities (4) and (5) raise at least two questions: *first, is it possible to set ε in them equal to zero, and second, if this is possible, how can we describe the sets of indices $\sigma = \{\sigma_0, \sigma_1, \dots, \sigma_{n-1}\}$, for which inequality (4) becomes an equality with $\varepsilon = 0$?*

The answer to the first question is negative; it follows from the following simple remark. Let the set \mathcal{A} consist of one square matrix A . Then by the well-known Gelfand formula (Horn and Johnson, 1985, Corollary 5.6.14) both values $\rho(\mathcal{A})$ and $\bar{\rho}(\mathcal{A})$ coincide with the spectral radius $\rho(A)$ of the matrix A . In this case, by reducing the matrix A to normal Jordan form, one can easily establish that the growth rate of the norms $\|A^n\|$ is of order $\rho(A)^n$ if and only if the eigenvalues of the matrix A that have the largest absolute value are semisimple. At the same time, for the case when at least one such eigenvalue of the matrix A is not semisimple, the growth rate of the norms $\|A^n\|$ is of order $p(n)\rho(A)^n$, where $p(t)$ is a polynomial.

The answer to the first question has another nuance: Even in cases where the growth rate of the norms of the matrix products $\|A_{\sigma_{n-1}} \cdots A_{\sigma_1} A_{\sigma_0}\|$ for a particular choice of the sequence of indices $\{\sigma_0, \sigma_1, \dots, \sigma_{n-1}\} \in \{0, \dots, m-1\}^n$ may coincide with $\rho(\mathcal{A})^n$, this may not happen for all norms of $\|\cdot\|$ but only for a particular choice of the corresponding norm. Moreover, even in the case of sets of matrices \mathcal{A} consisting of a single matrix, the construction of the corresponding norm turns out to be a nontrivial problem!

However, even in the simplest nontrivial case, when the set of matrices \mathcal{A} consists of a pair of matrices of dimension 2×2 , the question posed turns out to be much more complicated than the analysis of the growth rate of the norms of degrees $\|A^n\|$ of one matrix A . More precisely, unlike the corresponding analysis for one matrix, in the general case the computation of the maximal growth rate of the norms $\|A_{\sigma_n} \cdots A_{\sigma_1} A_{\sigma_0}\|$ turns out to be algebraically impossible (Kozyakin, 1990, 2003, 2013b), and the approximate computation of the corresponding rate turns out to be NP-hard (Blondel and Tsitsiklis, 2000; Tsitsiklis and Blondel, 1997).

Nevertheless, in a fairly general situation, a theoretically satisfactory answer to the first question can still be obtained. Recall that a set of matrices \mathcal{A} is called *irreducible* if matrices from \mathcal{A} have no common invariant subspaces other than $\{0\}$ and \mathbb{R}^d . The irreducibility of a set of matrices plays the same role in studying the growth rate of the norms of matrix products with multiple matrix factors as the semisimplicity of the eigenvalues with the largest absolute value of a single matrix plays in studying the growth rate of the norms of its powers. The approach proposed by N. Barabanov in (Barabanov, 1988a,b,c) proved to be the most fruitful here, and it has been further developed in several papers, from which we single out (Wirth, 2002).

¹Here and in the following $\rho(A)$, where A is a matrix, denotes the spectral radius of this matrix, i.e. the maximum of the absolute values of the eigenvalues of the matrix A .

Barabanov's Theorem. *If the set of matrices $\mathcal{A} = \{A_0, \dots, A_{m-1}\}$ is irreducible, then the number ρ is the joint (generalized) spectral radius of the set \mathcal{A} if and only if there exists a norm $\|\cdot\|$ in \mathbb{R}^d such that*

$$\rho\|x\| = \max \{\|A_0x\|, \|A_1x\|, \dots, \|A_{m-1}x\|\}, \quad \forall x \in \mathbb{R}^d. \quad (6)$$

A norm satisfying (6) is usually called the *Barabanov norm* corresponding to the set of matrices \mathcal{A} . This theorem does not provide a constructive description of Barabanov norms. Nevertheless, it turns out to be very effective in analyzing the growth of matrix products. In particular, it follows from Barabanov's Theorem that for irreducible sets of matrices \mathcal{A} , for every finite sequence of indices $\sigma = \{\sigma_0, \sigma_1, \dots, \sigma_{n-1}\} \in \{0, \dots, m-1\}^n$, in the Barabanov norm the inequality

$$\|A_{\sigma_{n-1}} \cdots A_{\sigma_1} A_{\sigma_0}\| \leq \rho(\mathcal{A})^n$$

holds, and that there is an infinite sequence of indices $\sigma = \{\sigma_0, \sigma_1, \dots\}$ such that for every n the equality

$$\|A_{\sigma_{n-1}} \cdots A_{\sigma_1} A_{\sigma_0}\| = \rho(\mathcal{A})^n$$

holds. So for irreducible sets of matrices there are much stronger statements than inequalities (4) and (5).

The second question, *how to describe sets of indices $\sigma = \{\sigma_0, \sigma_1, \dots, \sigma_{n-1}\}$, for which inequality (4) turns into equality when $\varepsilon = 0$* , is much more complicated than the first. The answer is currently known either in trivial (and therefore theoretically uninteresting) situations or in some special and rather restrictive cases. The answer to this question (as of the current understanding of the problem) is closely related to the concept of extremal trajectories of sets of matrices, which we briefly recall in the next section.

3. EXTREMAL TRAJECTORIES

In stating the main facts of this section we shall, as in the preceding section, adhere to the works (Kozyakin, 2005a,b, 2007). Additional discussion of the problems and statements involved can also be found in (Jungers, 2009).

The question of the growth rate of matrix products with factors from a certain set of matrices \mathcal{A} is closely related to a similar question of the growth rate of solutions of the difference equation (1) for all possible choices of index sequences $\{\sigma_n\}$ and initial values x_0 . The solutions $\{x_n\}$ of equation (1) will also be called the *trajectories* defined by the set of matrices \mathcal{A} , or simply the trajectories of the set of matrices \mathcal{A} . Since, according to (2), each element x_n of the trajectory $\{x_n\}$ can be represented as

$$x_n = A_{\sigma_{n-1}} \cdots A_{\sigma_1} A_{\sigma_0} x_0,$$

then due to (4)

$$\|x_n\| \leq \|A_{\sigma_{n-1}} \cdots A_{\sigma_1} A_{\sigma_0}\| \|x_0\| \leq e^{(\rho(\mathcal{A})+\varepsilon)n} \|x_0\|$$

for all sufficiently large n .

A trajectory $\{x_n\}$ of the set of matrices \mathcal{A} was called *characteristic* in (Kozyakin, 2005a,b, 2007) if it satisfies the inequalities

$$c_1 \rho^n(\mathcal{A}) \leq \|x_n\| \leq c_2 \rho^n(\mathcal{A}), \quad n = 0, 1, 2, \dots,$$

for some choice of constants $c_1, c_2 \in (0, \infty)$. In other words, by characteristic trajectories are meant those trajectories which, in the natural sense, are uniformly comparable to the sequence $\{\rho^n(\mathcal{A})\}$ on the whole infinite interval $n = 0, 1, 2, \dots$ of the variation of their indices. Note that the definition of the characteristic trajectory does not depend on the choice of the norm $\|\cdot\|$ in the space \mathbb{R}^d .

An important special case of characteristic trajectories is the so-called extremal trajectories. A trajectory $\{x_n\}$ of a collection of matrices \mathcal{A} will be called *extremal* if in some Barabanov norm $\|\cdot\|$ it satisfies the identity

$$\rho^{-n}(\mathcal{A}) \|x_n\| \equiv \text{const}. \quad (7)$$

As mentioned in Section 2, there are Barabanov norms for any irreducible set of matrices. Then, for any irreducible set of matrices, there are also extremal trajectories and hence characteristic

trajectories. For the proof, it suffices to construct the trajectory $\{x_n\}$ of the set of matrices $\mathcal{A} = \{A_0, \dots, A_{m-1}\}$, satisfying the initial condition $x_0 = x$, recursively. Let the element x_n have already been formed. Then, according to the definition of the Barabanov norm, the equality

$$\rho(\mathcal{A})\|x_n\| = \max \{\|A_0x_n\|, \|A_1x_n\|, \dots, \|A_{m-1}x_n\|\}$$

holds. Therefore, there exists an index σ_n such that

$$\rho(\mathcal{A})\|x_n\| = \|A_{\sigma_n}x_n\|,$$

and for condition (7) to be satisfied, it suffices to define the element x_{n+1} by the equality $x_{n+1} = A_{\sigma_n}x_n$.

Unlike the definition of a characteristic trajectory, the definition of an extremal trajectory depends on the choice of an extremal norm: A trajectory that is extremal in one norm may not be extremal in another norm. Nevertheless, for an irreducible set of matrices, there are always *universal extremal trajectories* in a certain sense, i.e., trajectories which are extremal with respect to any extremal norm: As shown in (Kozyakin, 2007, Th. 3), every limit point of every normed characteristic trajectory $\{x_n/\|x_n\|\}$ serves as the initial value of a trajectory which is automatically extremal in every Barabanov norm.

The description of extremal trajectories includes, besides the sequence $\mathbf{x} = \{x_n\}$, the index sequence $\{\sigma_n\}$, which is used to obtain the trajectory $\{x_n\}$ according to (1). In the following, we describe a construction that allows to define extremal trajectories as all possible trajectories of a multivalued nonlinear dynamical system, thus dispensing with the explicit description of the index sequence $\{\sigma_n\}$.

Let $\rho = \rho(\mathcal{A})$, and let $\|\cdot\|$ be a Barabanov norm corresponding to the set of matrices $\mathcal{A} = \{A_0, \dots, A_{m-1}\}$. For each $x \in \mathbb{R}^d$, we define the mapping $g(x)$ by

$$g(x) := \{w : \exists i \in \{0, \dots, m-1\} : w = A_i x, \text{ where } \|A_i x\| = \rho\|x\|\}. \quad (8)$$

By the definition of the Barabanov norm, for any $x \in \mathbb{R}^d$, the set $g(x)$ is nonempty and consists of at most m elements. Note that every mapping $g(x)$ has a closed graph and the identity

$$\|g(x)\| \equiv \rho\|x\| \quad (9)$$

holds for it.

Clearly, the sequence $\mathbf{x} = \{x_n\}$ is an extremal trajectory of the set of matrices \mathcal{A} in the Barabanov norm $\|\cdot\|$ if and only if it satisfies the inclusions

$$x_{n+1} \in g(x_n), \quad \forall n.$$

In other words, every trajectory of the multivalued mapping $g(\cdot)$ turns out to be an extremal trajectory of the set of matrices \mathcal{A} in the Barabanov norm $\|\cdot\|$. This gives rise to call the map $g(\cdot)$ a *generator of extremal trajectories*. Just like the Barabanov norm, the map $g(\cdot)$ cannot be stated explicitly in the general case. Nevertheless, a rather detailed description of the properties of generators of extremal trajectories can be obtained for two-element (i.e., $m = 2$) sets of nonnegative 2×2 matrices. Let us describe the corresponding constructions in detail.

We fix in space \mathbb{R}^2 a Barabanov norm $\|\cdot\|$ corresponding to the set of matrices $\mathcal{A} = \{A_0, A_1\}$. Let us define the sets

$$X_0 = \{x : \|A_0x\| = \rho\|x\|\}, \quad X_1 = \{x : \|A_1x\| = \rho\|x\|\}. \quad (10)$$

Each of these sets is closed, conic (i.e., it contains, together with the vector $x \neq 0$, each vector of the form tx , where $t \geq 0$), and by the definition of the Barabanov norm $X_0 \cup X_1 = \mathbb{R}^2$. In this case, the generator of extremal trajectories $g(\cdot)$ (see (8)) in the norm $\|\cdot\|$ takes the form

$$g(x) = \begin{cases} A_0x & \text{for } x \in X_0 \setminus X_1, \\ A_1x & \text{for } x \in X_1 \setminus X_0, \\ \{A_0x, A_1x\} & \text{for } x \in X_0 \cap X_1. \end{cases} \quad (11)$$

Let us examine more closely the structure of the mapping $g(\cdot)$. Let (r, φ) be the polar coordinates of the vector $x \in \mathbb{R}^2$. We denote by Ω_0 and Ω_1 the angular projections of the conic sets X_0 and X_1 , respectively. As mentioned above (see (9)), the mapping $g(\cdot)$ satisfies the identity

$\|g(x)\| \equiv \|x\|$. Thus, in the polar coordinate system (r, φ) , the mapping g has the form of a mapping with separable variables

$$g : (r, \varphi) \mapsto (\rho r, \Phi(\varphi)), \quad (12)$$

where $\rho = \rho(\mathcal{A})$ and

$$\Phi(\varphi) = \begin{cases} \Phi_0(\varphi) & \text{for } \varphi \in \Omega_0, \\ \Phi_1(\varphi) & \text{for } \varphi \in \Omega_1, \\ \{\Phi_0(\theta), \Phi_1(\theta)\} & \text{for } \varphi \in \Omega_0 \cap \Omega_1. \end{cases} \quad (13)$$

Here the functions $\Phi_0(\varphi)$ and $\Phi_1(\varphi)$ are explicitly defined as the angular coordinates of the mappings A_0x and A_1x , when $x = (r, \varphi)$ in polar coordinates.

The angular coordinate φ characterizes the direction of the vector $x = (r, \varphi)$. Accordingly, it is natural to interpret $\Phi(\varphi)$, $\varphi \in [0, 2\pi)$, as a *direction function* or *angular function* of the generator of extremal trajectories $g(\cdot)$. Note also that the function $\Phi(\varphi)$, while 2π -periodic, is in general not continuous. And since it is obtained as a result of taking the angular coordinates of linear mappings, its value modulo π , the function

$$\tilde{\Phi}(\varphi) = \Phi(\varphi) \bmod \pi, \quad \varphi \in [0, \pi), \quad (14)$$

is a π -periodic function.

From the definition (8) of the function $g(\cdot)$ and its representation in the form (12) we obtain the following description of extremal trajectories (Kozyakin, 2007, Lemma 6).

Lemma 1. *The nonzero trajectory $\{x_n\}$ is extremal for the set of 2×2 matrices $\mathcal{A} = \{A_0, A_1\}$ in the Barabanov norm $\|\cdot\|$ if and only if its elements in the polar coordinate system (r, φ) are representable as $x_n = (\rho^n r_0, \varphi_n)$, where ρ is the joint/generalized spectral radius of the set of matrices \mathcal{A} , and $\{\varphi_n\}$ is the trajectory of the multivalued mapping $\Phi(\cdot)$, i.e.*

$$\varphi_{n+1} \in \Phi(\varphi_n), \quad n = 0, 1, \dots$$

Moreover, the trajectory $\{x_n\}$ satisfies the equations

$$x_{n+1} = A_{\sigma_n} x_n, \quad n = 0, 1, \dots,$$

with some index sequence $\{\sigma_n\}$ if and only if the trajectory $\{\varphi_n\}$ satisfies the equations

$$\varphi_{n+1} = \Phi_{\sigma_n}(\varphi_n), \quad n = 0, 1, \dots,$$

or, which is equivalent, when the trajectory $\{\tilde{\varphi}_n\}$ with elements

$$\tilde{\varphi}_n = \varphi_n \bmod \pi, \quad n = 0, 1, \dots,$$

satisfies the equations

$$\tilde{\varphi}_{n+1} = \tilde{\Phi}_{\sigma_n}(\tilde{\varphi}), \quad n = 0, 1, \dots$$

4. A PAIR OF NONNEGATIVE MATRICES

Despite the fact that the Barabanov norm $\|\cdot\|$ is, as a rule, not known explicitly, the angular function $\Phi(\varphi)$ of the generator of extremal trajectories $g(\cdot)$ turns out in some cases to be defined “unambiguous enough.” In this context, we recall some constructions and results from (Kozyakin, 2005b, 2007) developed to construct one of the counterexamples to the so-called Finiteness Conjecture (Blondel et al., 2003; Bousch and Mairesse, 2002; Lagarias and Wang, 1995).

Consider the set of matrices $\mathcal{A} = \{A_0, A_1\}$, where

$$A_0 = \alpha \begin{bmatrix} a & b \\ 0 & 1 \end{bmatrix}, \quad A_1 = \beta \begin{bmatrix} 1 & 0 \\ c & d \end{bmatrix}. \quad (15)$$

For this set of matrices in (Kozyakin, 2005b, 2007) it was possible to perform a detailed analysis of the structure of the extremal trajectories under the additional assumptions that $\alpha, \beta > 0$ and

$$bc \geq 1 \geq a, d > 0.$$

In this paper, the approximate construction of the Barabanov norms of the sets of the matrix sets (15) (and the visualization of their unit spheres) were carried out using the algorithms and programs described in Section 6. An example of the unit sphere of the Barabanov norm for the

set of matrices (15), one of the extremal trajectories, and the corresponding angular function $\tilde{\Phi}(\varphi)$ for the case

$$\alpha = 0.576, \quad \beta = 0.8, \quad a = d = 0.9, \quad b = 1.1, \quad c = 1, \quad (16)$$

is shown in Fig. 1a. Here the black solid line represents the unit sphere of the Barabanov norm, i.e., the set of points $x \in \mathbb{R}^2$ for which $\|x\| = 1$ holds. Dotted and dashed lines denote the sets of points $x \in \mathbb{R}^2$ for which $\|A_0x\| = \rho$ and $\|A_1x\| = \rho$, respectively, where $\rho = \rho(\mathcal{A})$ is the joint/generalized spectral radius of the matrix set \mathcal{A} . Dash-dotted lines denote straight lines consisting of points $x \in X_0 \cap X_1$ (see (10)), i.e., points satisfying the equality $\|A_0x\| = \|A_1x\|$. Figure 1b shows the trajectory with the maximum rate of increase of the Barabanov norm $\|\cdot\|$. The construction of the next point of the trajectory x_{n+1} depends on which of the sectors bounded by straight dash-dotted lines the point x_n belongs to; the type of matrix used for this, A_0 or A_1 , is indicated in the shaded areas of Fig. 1b. The numerical analysis performed shows that $\rho(\mathcal{A}) \approx 1.098668$ and the index sequence $\{\sigma_n\}$ of the extremal trajectory shown in Fig. 1b is of the form²

$$\{\sigma_n\} = 10110110101101101101101101101101101101101101101101 \dots, \quad (17)$$

where on sufficiently large segments (words) of the sequence $\{\sigma_n\}$ of length 10000 the symbol **0** occurs with a frequency of ≈ 0.364 and the symbol **1** occurs with a frequency of ≈ 0.636 . The index sequence $\{\sigma_n\}$ was constructed with the program `barnorm_sturm.py` by computing point iterations using the angular function $\tilde{\Phi}(\varphi)$, as shown in Figs. 1c and 2. In these figures, the thick solid lines denote sections of the graphs of the functions $\Phi_0(\varphi)$ and $\Phi_1(\varphi)$ through which, according to (13)–(14) the function $\tilde{\Phi}(\varphi)$ is determined, and thin dashed lines mark those sections of the graphs of the functions $\Phi_0(\varphi)$ and $\Phi_1(\varphi)$ that were discarded in the definition of the function $\tilde{\Phi}(\varphi)$.

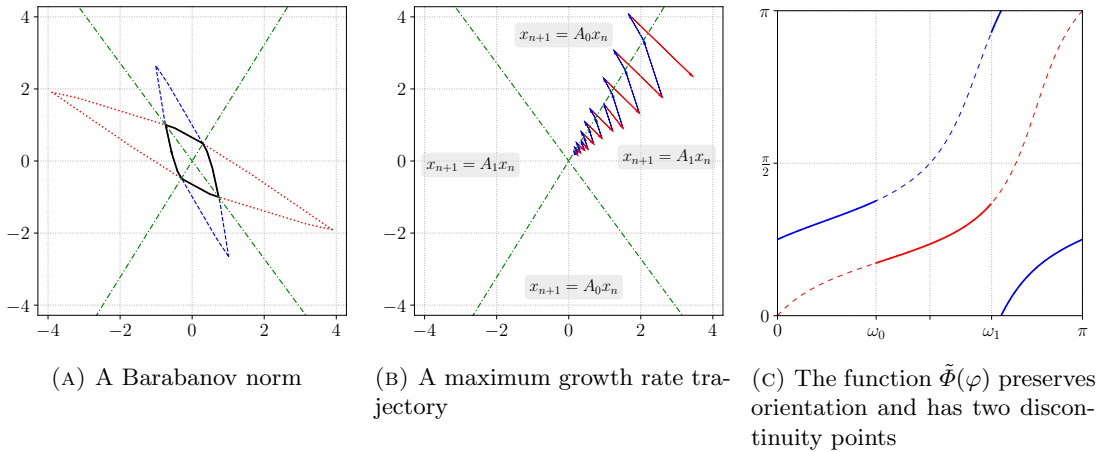


FIGURE 1. A Barabanov norm and the angular function for the set of matrices (15), where $\alpha = 0.576$, $\beta = 0.8$, $a = d = 0.9$, $b = 1.1$, $c = 1$

In this case, the fact that both matrices A_0 and A_1 are nonnegative and therefore leave the first quadrant in \mathbb{R}^2 invariant proved to be of fundamental importance for the theoretical study of the structure of extremal trajectories carried out in (Kozyakin, 2005b, 2007). The latter fact is reflected in the observation that the angular function $\tilde{\Phi}(\varphi)$ in this case maps the segment $[0, \frac{\pi}{2})$ into itself, which simplifies the study of its trajectories $\{\tilde{\varphi}_n\}$. In particular, it was proved in (Kozyakin, 2005b, 2007) that the restrictions of the sets Ω_0 and Ω_1 in (13) on $[0, \frac{\pi}{2})$ are segments with a single common point ω_0 . As numerical calculations show, in the case (16) we are considering, these sets are as follows:

$$\Omega_0 \cap [0, \frac{\pi}{2}) = [\omega_0, \frac{\pi}{2}), \quad \Omega_1 \cap [0, \frac{\pi}{2}) = [0, \omega_0).$$

²In the theory of symbolic sequences, it is customary to write the elements of the corresponding sequences in a row without intermediate separators.

Accordingly, the function $\tilde{\Phi}(\varphi)$ in our case has only one discontinuity point ω_0 on the segment $[0, \frac{\pi}{2})$, see Fig. 2.

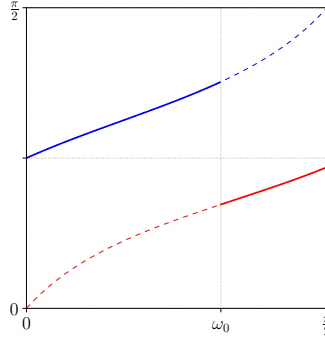


FIGURE 2. The angular function $\tilde{\Phi}(\varphi)$, $\varphi \in [0, \frac{\pi}{2})$, for the set of matrices (15)

If we treat $\varphi \in [0, \frac{\pi}{2})$ as an angular coordinate on a circle of length $\frac{\pi}{2}$, we can take $\tilde{\Phi}(\varphi)$ as an orientation-preserving mapping³ of the corresponding circle into itself, see (Kozyakin, 2005b, 2007) for details. In this case, as shown in (Kozyakin, 2005b, 2007), the index sequence $\{\sigma_n\}$ of each trajectory $\tilde{\varphi}_n$ of the mapping $\tilde{\Phi}$ turns out to be either periodic or the so-called *Sturmian* (see, e.g., (Fogg, 2002, Ch. 6), (Lothaire, 2002, Ch. 2)).

Currently, there are several definitions of the Sturmian sequences. One of the simplest analytic definitions states that a Sturmian sequence is an integer sequence $\{\sigma_n\}$, which for all integer n is defined by the relations

$$\sigma_n = [(n+1)\theta + \eta] - [n\theta + \eta],$$

where $\theta \in (0, 1)$ is an irrational number, $\eta \in \mathbb{R}$, and $[\cdot]$ denotes the integer part of the number. The following equivalent definition will be more useful for us: let $\{\varphi_n\}$ be a trajectory running on a circle of length 1 (or, equivalently, on the interval $[0, 1)$) through the rotation map

$$\varphi_{n+1} = \varphi_n + \theta \bmod 1, \quad (18)$$

where θ is an irrational number. We associate the index sequence $\{\sigma_n\}$ with this trajectory and set (see Fig. 3a)

$$\sigma_n = \begin{cases} 0, & \text{if } \varphi_n \in I_0 := [\theta, 1), \\ 1, & \text{if } \varphi_n \in I_1 := [0, \theta). \end{cases} \quad (19)$$

Then the resulting sequence $\sigma = \{\sigma_n\}$ (which is not periodic due to the irrationality of θ) is simply the so-called Sturmian sequence formed by the symbol pair $\{0, 1\}$ and the “rotation number” θ . In defining Sturmian sequences, we will later give up the requirement that the number θ must be irrational. This will lead to the fact that such generalized Sturmian sequences may turn out to be periodic.

We also note that the characteristic property of Sturmian sequences σ with irrational θ is that they satisfy the identity

$$p(n, \sigma) \equiv n + 1, \quad (20)$$

where $p(n, \sigma)$ is the so-called *subword complexity function*, defined as the number of distinct words of length n in the sequence σ , see, e.g., (Lothaire, 2002, Sec. 1.2.2), (Fogg, 2002, Sec. 5.1.3), (Berstel and Karhumäki, 2003, Sec. 6).

One of the most important properties of the Sturmian sequences is the following fact (Fogg, 2002, Lemma 6.1.3):

³The mapping $f(\varphi)$ of a circle into itself is called *orientation-preserving* if for any triple of points $\varphi_0, \varphi_1, \varphi_2$ on the circle the order of these points in going round the circle in any direction agrees with the order of their images $f(\varphi_0), f(\varphi_1), f(\varphi_2)$ when going around the circle in the same direction.

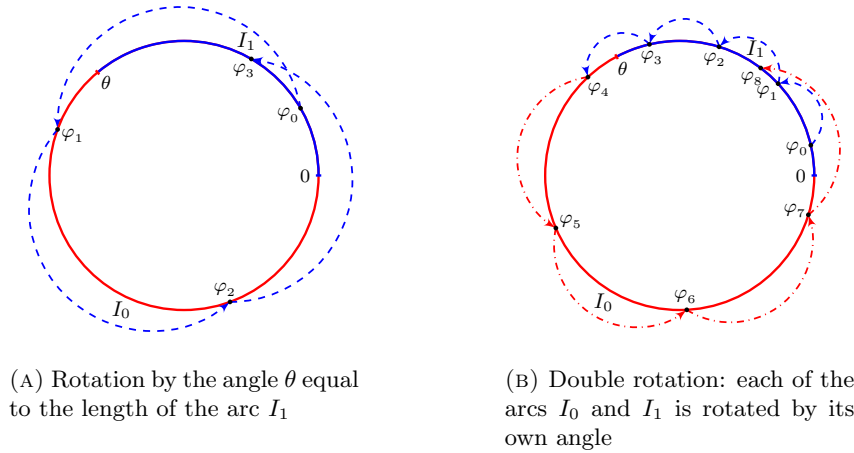


FIGURE 3. Regular and double rotation of a circle

Lemma 2. *In any (generalized) Sturmian sequence consisting of two characters $\{0, 1\}$, exactly one of the symbol sequences (words) **00** or **11** does not occur.*

Lemma 2 becomes clear if we note that the points $\{\varphi_n\}$ satisfying (18) cannot fall twice in succession in the interval $[0, \theta)$ or $[\theta, 1)$ which has the smallest length.

For illustration, note that *the Sturmian index sequence (17) does not contain the symbol sequence (word) 00.*

5. A PAIR OF MATRICES SIMILAR TO PLANE ROTATIONS

As mentioned in Section 4, previous studies (Blondel et al., 2003; Bousch and Mairesse, 2002; Kozyakin, 2005b, 2007; Lagarias and Wang, 1995) for matrix sets (15) consisting of nonnegative matrices of a special form have provided some clarity on the structure of index sequences that yield the maximal growth rate of matrix product norms. For this reason, in this section we focus on considering less studied matrix sets, namely sets consisting of matrices that may have negative elements. Our goal is to give an example of matrix sets $\mathcal{A} = \{A_0, A_1\}$ consisting of matrices of dimension 2×2 , in which the sequences of indices $\{\sigma_i\}$ maximizing $\|A_{\sigma_n} \cdots A_{\sigma_1} A_{\sigma_0} x\|$, where $\|\cdot\|$ is a Barabanov norm, *are not Sturmian!* One of the simplest types of this kind of matrix sets is the set of matrices $\mathcal{A} = \{A_0, A_1\}$, where

$$A_0 = \begin{bmatrix} \cos \theta_0 & -\sin \theta_0 \\ \sin \theta_0 & \cos \theta_0 \end{bmatrix}, \quad A_1 = \begin{bmatrix} \cos \theta_1 & -\lambda \sin \theta_1 \\ \frac{1}{\lambda} \sin \theta_1 & \cos \theta_1 \end{bmatrix}. \quad (21)$$

Further considerations in this section are based on computational experiments and have no theoretical basis at this time. In this respect, this section should be considered as a kind of set of questions (with accompanying comments) for further research.

Consider the sets of matrices $\mathcal{A} = \{A_0, A_1\}$ defined by the following parameters:

$$\text{Case 1 : } \theta_0 = 0.4, \quad \theta_1 = 0.8, \quad \lambda = 0.75,$$

$$\text{Case 2 : } \theta_0 \approx 0.6151, \quad \theta_1 = 0.8, \quad \lambda = 0.75,$$

$$\text{Case 3 : } \theta_0 = 0.7, \quad \theta_1 = 0.8, \quad \lambda = 0.75.$$

In these cases, the software tools described in Section 6 allowed not only to visualize approximately the shape of the unit sphere of the Barabanov norm, but also to show examples of iterations $x_{n+1} = A_{\sigma_n} x_n$ where the maximum growth rate of the Barabanov norm of $\|x_n\|$ is reached. It also approximately finds the angular function $\tilde{\Phi}(\varphi)$ (see (14)) of the matrix set \mathcal{A} , whose iterations allow the computation of the angular coordinates $\tilde{\varphi}_n$ of the corresponding vectors x_n , without computing their norms! The results of the corresponding numerical simulations are shown in Figs. 4, 5 and 6. Since the meaning of the notation in these figures repeats verbatim the explanations made for Figs. 1a, 1b and 1c, we do not present them here.

As can be seen in Figs. 4a, 5a, and 6a, in all three cases the set $X_0 \cap X_1$ (see definitions in (10), (11)) turns out to be the union of two straight lines passing through the origin (dash-dotted lines). In this context, the following question arises.

Question 1. For the case of a pair of nonnegative matrices (15), the statement that the part of the set $X_0 \cap X_1$ passing through the first and third quadrants is a straight line is strictly justified in (Kozyakin, 2005b, 2007). We are not aware of such a proof for the sets of matrices (21) considered in this section. The question arises: **Is the set $X_0 \cap X_1$ in this case always the union of two straight lines? And why only of two?** \square

From Figs. 4b, 5b, and 6b it is evident (and it was calculated with the program `barnorm_rot.py` described in Section 6) that the index sequences of the trajectories with the maximum growth rate in the Barabanov norm, for Cases 1–3, are as follows:

$$\begin{aligned}\{\sigma_n\} &= 10000110000110000110001100001100001100001100001100\dots, \\ \{\sigma_n\} &= 10001100110001100110001100110001100110001100110001\dots, \\ \{\sigma_n\} &= 100110011001100011001100110011001100110011001100011001\dots.\end{aligned}$$

Calculations with the program `barnorm_rot.py` have shown that in sequences $\{\sigma_n\}$ of length 10000 the symbols **0**, **1**, **00**, **01**, **10** and **11** occur with the following frequencies:

Symbols	0	1	00	01	10	11
Frequencies (Case 1)	0.655	0.345	0.483	0.172	0.172	0.172
Frequencies (Case 2)	0.555	0.445	0.333	0.222	0.222	0.222
Frequencies (Case 3)	0.517	0.483	0.276	0.241	0.241	0.241

From this, according to Lemma 2, the following fundamentally important conclusion follows.

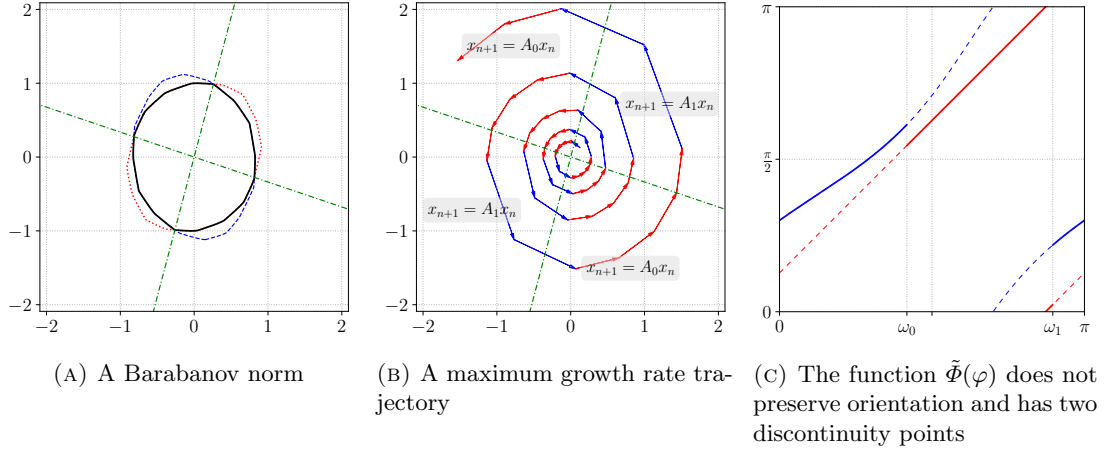


FIGURE 4. A Barabanov norm and the angular function: Case 1

Main Claim. In the cases of pairs of matrices (21), similar to plane rotations, the index sequences of trajectories with the maximal growth rate in the Barabanov norm **are not (generalized) Sturmian**.

Let us turn to a more detailed analysis of the obtained results of numerical simulation.

Case 1. As can be seen from Fig. 4c, in Case 1 the angular function $\tilde{\Phi}(\varphi)$, considered as a mapping of the circle into itself, **does not preserve orientation**. In particular, this situation resembles the behavior of the so-called *double rotations* (Artigiani et al., 2021; Clack, 2013; Kryzhevich, 2020; Suzuki et al., 2005), defined by the equation

$$f_{\theta_1, \theta_2, \theta}(\varphi) = \begin{cases} \varphi + \theta_1 \bmod 1 & \text{for } x \in [0, \theta), \\ \varphi + \theta_2 \bmod 1 & \text{for } x \in [\theta, 1), \end{cases} \quad (22)$$

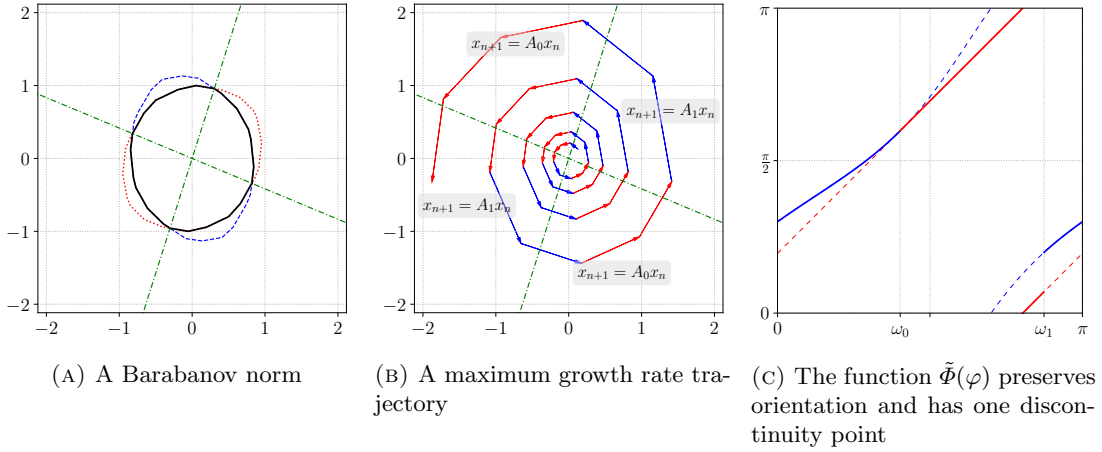


FIGURE 5. A Barabanov norm and the angular function: Case 2

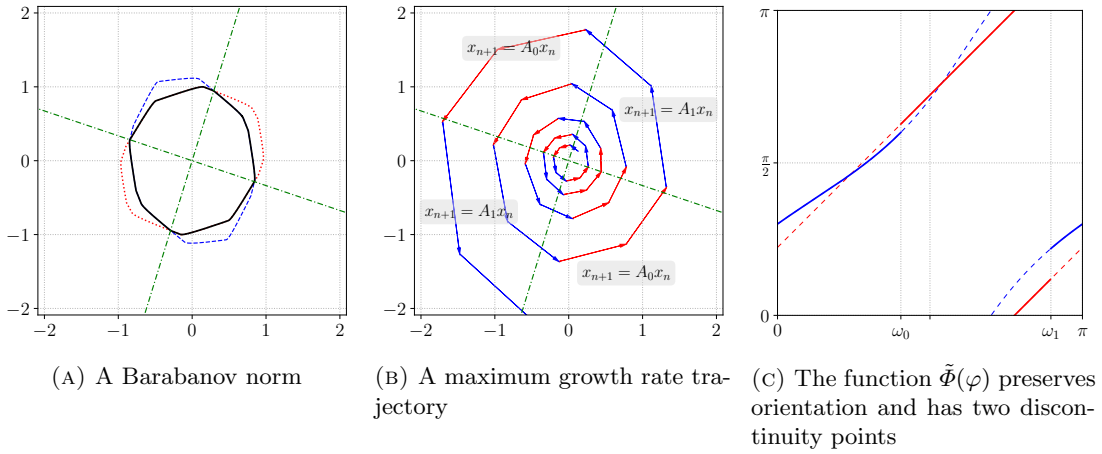


FIGURE 6. A Barabanov norm and the angular function: Case 3

where $(\theta_1, \theta_2, \theta) \in [0, 1) \times [0, 1) \times [0, 1)$ are some parameters (see the example in Fig. 3b).

The mappings $\tilde{\Phi}(\varphi)$ and $f_{\theta_1, \theta_2, \theta}(\varphi)$ are related by the fact that both are not continuous and do not preserve orientation on a circle but their action is determined by some “rotations” on two continuity intervals of the mappings. The difference between the angular function $\tilde{\Phi}(\varphi)$ from the double rotations of the circle $f_{\theta_1, \theta_2, \theta}(\varphi)$ is that for the first of these mappings, the rotation angles are not constant, while in the case of the mapping $f_{\theta_1, \theta_2, \theta}(\varphi)$, the rotation angles are constant for each of the intervals $[0, \theta)$ and $[\theta, 1)$. Double rotations of the circle are thus somewhat easier to study, and some progress has been made recently in their analysis (Artigiani et al., 2021; Clack, 2013; Suzuki et al., 2005).

Question 2. Is it possible (by analogy with the case of the angular function $\tilde{\Phi}(\varphi)$ for the set of nonnegative matrices (15)) for the angular function $\tilde{\Phi}(\varphi)$, arising in Case 1, select parameters $\theta_1, \theta_2, \theta$ such that the corresponding index sequences for the mapping $\tilde{\Phi}(\varphi)$ would match the index sequences for the mapping $f_{\theta_1, \theta_2, \theta}(\varphi)$? \square

A positive answer to this question does not seem very likely. As a first step to clarify the situation, it would be possible to compare the frequencies of occurrence of the symbols $\mathbf{0}$ and $\mathbf{1}$, as well as groups of consecutive identical symbols $\mathbf{00} \dots \mathbf{0}$ and $\mathbf{11} \dots \mathbf{1}$ in index sequences for the mappings $\tilde{\Phi}(\varphi)$ and $f_{\theta_1, \theta_2, \theta}(\varphi)$. Perhaps a negative answer to Question 2 could have been obtained already at this stage.

Question 3. Again by analogy with the case of the angular function $\tilde{\Phi}(\varphi)$ for the set of matrices (15): For the angular function $\tilde{\Phi}(\varphi)$ occurring in Case 1, are there limit frequencies for the occurrence of the symbols **0** and **1** in index sequences $\{\sigma_n\}$? If the answer is yes, do these frequencies depend on a particular index sequence or not (as in the case of the angular function $\tilde{\Phi}(\varphi)$ for the matrix set (15))? \square

Question 4. If Question 3 is answered in the affirmative, then are the limiting frequencies of occurrence of the symbols **0** and **1** in the index sequences $\{\sigma_n\}$ for the angular function $\tilde{\Phi}(\varphi)$ dependent on a particular index sequence or not (as in the case of the angular function $\tilde{\Phi}(\varphi)$ for a set of matrices (15))? \square

In answering Question 4, it might be useful to refer to the theory of circle mappings (Alsedà and Mañosas, 1990, 1996; Alsedà and Moreno, 2000; Misiurewicz, 1986, 2007), both continuous and discontinuous, which are not orientation-preserving. Unfortunately, the lack of the orientation preserving property makes the analysis of the mappings of the circle much more difficult. Instead of characterizing the “mean rotation angle” in such mappings by the so-called “rotation number” (a standard tool in the theory of orientation-preserving circle mappings), the concept of a “rotation interval” emerges in non-orientation-preserving circle mappings (Alsedà and Mañosas, 1990; Alsedà and Moreno, 2000; Misiurewicz, 1986, 2007). The latter fact may be crucial in answering the question whether the frequency of occurrence of symbols in an index sequence depends on that sequence. Note, however, that in our numerical experiments the dependence of the frequency characteristics on the trajectory was not observed.

Cases 2 and 3. In these cases the angular function $\tilde{\Phi}(\varphi)$, considered as a mapping of the circle into itself, **preserves orientation**. In Case 2 it has one discontinuity point and in Case 3 two, see Figs. 5c and 6c. Therefore (Kozyakin, 2005a,b, 2007), for the mapping $\tilde{\Phi}(\varphi)$ in these cases, the so-called *rotation number* $\varkappa(\tilde{\Phi})$ is defined, which characterizes the “mean rotation angle” performed by this mapping.

In the case where $\tilde{\Phi}(\varphi)$ is an angular function (12) generated by the pair of nonnegative matrices (15), the rotation number $\varkappa(\tilde{\Phi})$ coincides with the frequency of hitting the trajectory elements

$$x_{n+1} = A_{\sigma_n} x_n, \quad n = 0, 1, \dots,$$

into the set X_0 , and hence with the frequency of occurrence of the symbol **0** in the corresponding index sequence.

Question 5. In Cases 2 and 3, as mentioned above, a rotation number is also defined for the mapping $\tilde{\Phi}(\varphi)$. However, whether this implies the existence of limiting frequencies for the occurrence of the symbols **0** and **1** in the index sequences $\{\sigma_n\}$ for the angular function $\tilde{\Phi}(\varphi)$ remains unclear! \square

The behavior of the mapping $\tilde{\Phi}(\varphi)$, considered as a mapping of a circle, resembles the behavior of the mapping of a circle (18) in Cases 2 and 3:

$$\varphi_{n+1} = \varphi_n + \theta \bmod 1, \quad (23)$$

with the difference that this time the index sequence $\{\sigma_n\}$ is not calculated using formula (19), but as follows:

$$\sigma_n = \begin{cases} 0, & \text{if } \varphi_n \in I_0 := [\theta_0, 1), \\ 1, & \text{if } \varphi_n \in I_1 := [0, \theta_0), \end{cases} \quad (24)$$

where the length of the interval I_1 is generally different from the angle of rotation: $\theta_0 \neq \theta$. As shown in (Berstel and Vuillon, 2002), the behavior of the index sequence (24) can be expressed in terms of a pair of Sturmian sequences generated by rotation through angle θ , but in a rather complex way.

A question similar to that of Question 2 may be asked here.

Question 6. For the angular function $\tilde{\Phi}(\varphi)$ occurring in Cases 2 and 3, is it possible to choose the parameters θ_0 and θ such that the corresponding index sequences for $\tilde{\Phi}(\varphi)$ coincide with the index sequences (24) for the rotation mapping (23)? \square

As in the case of Question 2, a positive answer to this question does not seem very likely. Here, as a first step to clarify the situation, one might compare the frequencies of occurrence of the symbols **0** and **1** as well as groups of consecutive identical symbols **00...0** and **11...1** in index sequences for the mappings $\tilde{\Phi}(\varphi)$ and (23)–(24). Note, however, that in this case (unlike the situation described in the discussion of Question 4) the computation of the frequency characteristics of the index sequences (24) can be performed theoretically, which is possible may simplify the research.

6. METHODS AND TOOLS FOR NUMERICAL MODELING

In this work, an approximate construction of Barabanov norms of matrix sets (and visualization of their unit spheres as well as the trajectories with the maximum growth rate in the Barabanov norm) was performed using the programs `barnorm_sturm.py` and `barnorm_rot.py`, which are available for download from the website <https://github.com/kozyakin/barnorm>. These programs use a small modification of the max-relaxation algorithm for the iterative construction of Barabanov norms, which can be found in (Kozyakin, 2010a, 2011). The modification compared to the software implementation of the corresponding algorithms described in (Kozyakin, 2010b) was that convex centrally symmetric polygons were chosen as unit spheres of norms approximating the Barabanov norm. The advantage of this approach over the approach of (Kozyakin, 2010b) is that when linear transformations are applied, the unit spheres of the norms $\|A_0x\|$ and $\|A_1x\|$ are again convex centrally symmetric polygons. Using the library `shapely` of the language `Python`, this allows the iterative computation of the norm $\max\{\|A_0x\|, \|A_1x\|\}$ without loss of precision for each iteration.

The programs `barnorm_sturm.py` and `barnorm_rot.py` differ from each other only in the specification of the matrices A_0 and A_1 and in the amount of graphical data displayed. Both programs are implemented in the Python programming language of versions 3.8–3.10 of the `Miniconda3` (`Anaconda3`) distribution.

For the convenience of the reader, a listing of the program `barnorm_rot.py` is provided in Appendix A.

7. CONCLUSION

The paper presents the results of a numerical simulation of the fastest growing (in the Barabanov norm) trajectories generated by sets of 2×2 matrices. The results obtained indicate that in certain situations the maximum growth rate can be achieved on trajectories with non-Sturmian sequences of indices, which makes these situations fundamentally different from most theoretical studies carried out so far in the theory of joint/generalized spectral radius.

Section 5 presents the results of the numerical simulations performed in this paper and formulates a number of open questions. In particular, it would be interesting to compare the complexity functions $p(n, \sigma)$ of the index sequences $\sigma = \{\sigma_n\}$ of the mappings $\tilde{\Phi}(\varphi)$ with the complexity functions of the index sequences of the “test” circle mappings (22) and (23)–(24). This question seems all the more interesting because, unlike Sturmian sequences for which the growth rate of the function $p(n, \sigma)$ is linear (see (20)), for sequences generated by the double rotation mappings (23)–(24), the growth rate of the complexity function can be superlinear: $p(n, \sigma) \sim n^\gamma$, where $\gamma > 1$ (Clack, 2013). An example of such a growth rate of the norms of matrix products is described in (Hare et al., 2013).

Since the bulk of the results presented above are numerical in nature, this paper should not be considered a full-fledged theoretical study but rather a plan for further research on the subject.

ACKNOWLEDGMENT

The author thanks Aljoša Peperko for pointing out some obscurities in the presentation.

REFERENCES

- Alsedà, L., Mañosas, F., 1990. Kneading theory and rotation intervals for a class of circle maps of degree one. *Nonlinearity* 3, 413–452. URL: <https://iopscience.iop.org/article/10.1088/0951-7715/3/2/008>.

- Alsedà, L., Mañosas, F., 1996. Kneading theory for a family of circle maps with one discontinuity. *Acta Math. Univ. Comenian. (N.S.)* 65, 11–22.
- Alsedà, L., Moreno, J.M., 2000. On the rotation sets for non-continuous circle maps. *Acta Math. Univ. Comenian. (N.S.)* 69, 115–125.
- Artigiani, M., Fougeron, C., Hubert, P., Skripchenko, A., 2021. A note on double rotations of infinite type. *ArXiv.org e-Print archive*. URL: <https://arxiv.org/abs/2102.11803>, doi:10.48550/arXiv.2102.11803, arXiv:2102.11803.
- Barabanov, N.E., 1988a. Lyapunov indicator of discrete inclusions. I. *Autom. Remote Control* 49, 152–157.
- Barabanov, N.E., 1988b. The Lyapunov indicator of discrete inclusions. II. *Autom. Remote Control* 49, 283–287.
- Barabanov, N.E., 1988c. The Lyapunov indicator of discrete inclusions. III. *Autom. Remote Control* 49, 558–565.
- Berger, M.A., Wang, Y., 1992. Bounded semigroups of matrices. *Linear Algebra Appl.* 166, 21–27. URL: <https://www.sciencedirect.com/science/article/pii/002437959290267E>, doi:10.1016/0024-3795(92)90267-E.
- Berstel, J., Karhumäki, J., 2003. Combinatorics on words—a tutorial. *Bull. Eur. Assoc. Theor. Comput. Sci. EATCS* 79, 178–228. URL: https://www.worldscientific.com/doi/abs/10.1142/9789812562494_0059, doi:10.1142/9789812562494_0059.
- Berstel, J., Vuillon, L., 2002. Coding rotations on intervals. *Theoret. Comput. Sci.* 281, 99–107. URL: <https://www.sciencedirect.com/science/article/pii/S0304397502000099>, doi:10.1016/S0304-3975(02)00009-9, arXiv:math/0106217.
- Bertsekas, D.P., Tsitsiklis, J.N., 1989. *Parallel and Distributed Computation. Numerical Methods*. Prentice Hall, Englewood Cliffs. NJ.
- Blondel, V.D., Canterini, V., 2003. Undecidable problems for probabilistic automata of fixed dimension. *Theory Comput. Syst.* 36, 231–245. URL: <https://link.springer.com/article/10.1007/s00224-003-1061-2>, doi:10.1007/s00224-003-1061-2.
- Blondel, V.D., Jungers, R., Protasov, V., 2006. On the complexity of computing the capacity of codes that avoid forbidden difference patterns. *IEEE Trans. Inform. Theory* 52, 5122–5127. URL: <https://ieeexplore.ieee.org/document/1715550>, doi:10.1109/TIT.2006.883615, arXiv:cs/0601036.
- Blondel, V.D., Theys, J., Vladimirov, A.A., 2003. An elementary counterexample to the finiteness conjecture. *SIAM J. Matrix Anal. Appl.* 24, 963–970 (electronic). URL: https://epubs.siam.org/sima/resource/1/sjmael/v24/i4/p963_s1, doi:10.1137/S0895479801397846.
- Blondel, V.D., Tsitsiklis, J.N., 2000. A survey of computational complexity results in systems and control. *Automatica J. IFAC* 36, 1249–1274. URL: <https://www.sciencedirect.com/science/article/pii/S0005109800000509>, doi:10.1016/S0005-1098(00)00050-9.
- Bousch, T., Mairesse, J., 2002. Asymptotic height optimization for topical IFS, Tetris heaps, and the finiteness conjecture. *J. Amer. Math. Soc.* 15, 77–111 (electronic). URL: <https://www.ams.org/journals/jams/2002-15-01/S0894-0347-01-00378-2/>, doi:10.1090/S0894-0347-01-00378-2.
- Brayton, R.K., Tong, C.H., 1979. Stability of dynamical systems: a constructive approach. *IEEE Trans. Circuits Syst.* 26, 224–234. URL: <https://ieeexplore.ieee.org/document/1084637>, doi:10.1109/TCS.1979.1084637.
- Chazan, D., Miranker, W., 1969. Chaotic relaxation. *Linear Algebra Appl.* 2, 199–222. URL: <https://www.sciencedirect.com/science/article/pii/0024379569900287>, doi:10.1016/0024-3795(69)90028-7.
- Clack, G., 2013. *Double Rotations*. Ph.D. thesis. University of Surrey (United Kingdom). Guildford. URL: <https://openresearch.surrey.ac.uk/esploro/outputs/doctoral/Double-Rotations/99511546402346>.
- Daubechies, I., Lagarias, J.C., 1992. Sets of matrices all infinite products of which converge. *Linear Algebra Appl.* 161, 227–263. URL: <https://www.sciencedirect.com/science/article/pii/002437959290012Y>, doi:10.1016/0024-3795(92)90012-Y.

- Daubechies, I., Lagarias, J.C., 2001. Corrigendum/addendum to: “Sets of matrices all infinite products of which converge” [Linear Algebra Appl. **161** (1992), 227–263; MR1142737 (93f:15006)]. Linear Algebra Appl. **327**, 69–83. URL: <https://www.sciencedirect.com/science/article/pii/S0024379500003141>, doi:10.1016/S0024-3795(00)00314-1.
- Fogg, N.P., 2002. Substitutions in dynamics, arithmetics and combinatorics. volume 1794 of *Lecture Notes in Mathematics*. Springer-Verlag, Berlin. URL: <https://link.springer.com/book/10.1007/b13861>, doi:10.1007/b13861. edited by V. Berthé, S. Ferenczi, C. Mauduit and A. Siegel.
- Hare, K.G., Morris, I.D., Sidorov, N., 2013. Extremal sequences of polynomial complexity. Math. Proc. Cambridge Philos. Soc. **155**, 191–205. URL: <https://dx.doi.org/10.1017/S0305004113000157>, doi:10.1017/S0305004113000157, arXiv:1201.6236.
- Heil, C., Strang, G., 1995. Continuity of the joint spectral radius: application to wavelets, in: Linear algebra for signal processing (Minneapolis, MN, 1992). Springer, New York. volume 69 of *IMA Vol. Math. Appl.*, pp. 51–61. doi:10.1007/978-1-4612-4228-4_4.
- Horn, R.A., Johnson, C.R., 1985. Matrix analysis. Cambridge University Press, Cambridge. doi:10.1017/CB09780511810817.
- Jungers, R., 2009. The joint spectral radius. volume 385 of *Lecture Notes in Control and Information Sciences*. Springer-Verlag, Berlin. URL: <https://link.springer.com/book/10.1007/978-3-540-95980-9>, doi:10.1007/978-3-540-95980-9. Theory and applications.
- Jungers, R.M., Protasov, V., Blondel, V.D., 2008. Efficient algorithms for deciding the type of growth of products of integer matrices. Linear Algebra Appl. **428**, 2296–2311. URL: <https://www.sciencedirect.com/science/article/pii/S0024379507003436>, doi:10.1016/j.laa.2007.08.001.
- Kozyakin, V., 2005a. A dynamical systems construction of a counterexample to the finiteness conjecture, in: Proceedings of the 44th IEEE Conference on Decision and Control, 2005 and 2005 European Control Conference. CDC-ECC’05., pp. 2338–2343. URL: <https://ieeexplore.ieee.org/document/1582511>, doi:10.1109/CDC.2005.1582511.
- Kozyakin, V., 2010a. Iterative building of Barabanov norms and computation of the joint spectral radius for matrix sets. Discrete Contin. Dyn. Syst. Ser. B **14**, 143–158. URL: <https://www.aims sciences.org/article/doi/10.3934/dcdsb.2010.14.143>, doi:10.3934/dcdsb.2010.14.143, arXiv:0810.2154.
- Kozyakin, V., 2010b. Max-Relaxation iteration procedure for building of Barabanov norms: Convergence and examples. ArXiv.org e-Print archive. URL: <https://arxiv.org/abs/1002.3251>, doi:10.48550/arXiv.1002.3251, arXiv:1002.3251.
- Kozyakin, V., 2011. A relaxation scheme for computation of the joint spectral radius of matrix sets. J. Differ. Equations Appl. **17**, 185–201. URL: <https://www.tandfonline.com/doi/abs/10.1080/10236198.2010.549008>, doi:10.1080/10236198.2010.549008, arXiv:0810.4230.
- Kozyakin, V., 2013a. An annotated bibliography on the convergence of matrix products and the theory of joint/generalized spectral radius. Preprint. Institute for Information Transmission Problems. Moscow. URL: <https://kozyakin.github.io/jsrbib/JSRbib.html>, doi:10.13140/RG.2.1.4257.5040/1.
- Kozyakin, V.S., 1990. Algebraic unsolvability of problem of absolute stability of desynchronized systems. Autom. Remote Control **51**, 754–759.
- Kozyakin, V.S., 2003. Indefinability in o-minimal structures of finite sets of matrices whose infinite products converge and are bounded or unbounded. Autom. Remote Control **64**, 1386–1400. URL: <https://link.springer.com/article/10.1023/A:1026091717271>, doi:10.1023/A:1026091717271.
- Kozyakin, V.S., 2005b. Rotation numbers of discontinuous orientation-preserving circle maps revisited. Information Processes **5**, 301–335. URL: <http://www.jip.ru/2005/283-300.pdf>.
- Kozyakin, V.S., 2007. Structure of extremal trajectories of discrete linear systems and the finiteness conjecture. Autom. Remote Control **68**, 174–209. URL: <https://link.springer.com/article/10.1134/S0005117906040171>, doi:10.1134/S0005117906040171.

- Kozyakin, V.S., 2013b. Algebraic unsolvability of problem of absolute stability of desynchronized systems revisited. ArXiv.org e-Print archive. URL: <https://arxiv.org/abs/1301.5409>, doi:10.48550/arXiv.1301.5409, arXiv:1301.5409.
- Kryzhevich, S., 2020. Invariant measures for interval translations and some other piecewise continuous maps. *Math. Model. Nat. Phenom.* 15, 15. URL: <https://www.mmnp-journal.org/articles/mmnp/abs/2020/01/mmnp180201>, doi:10.1051/mmnp/2019041.
- Lagarias, J.C., Wang, Y., 1995. The finiteness conjecture for the generalized spectral radius of a set of matrices. *Linear Algebra Appl.* 214, 17–42. URL: <https://www.sciencedirect.com/science/article/pii/0024379593000522>, doi:10.1016/0024-3795(93)00052-2.
- Lothaire, M., 2002. Algebraic combinatorics on words. volume 90 of *Encyclopedia of Mathematics and its Applications*. Cambridge University Press, Cambridge. URL: <https://www.cambridge.org/core/books/algebraic-combinatorics-on-words/F0C477102253C41503EB7D6AE7C0F367>, doi:10.1017/CB09781107326019.
- Maesumi, M., 1998. Calculating joint spectral radius of matrices and Hölder exponent of wavelets, in: *Approximation theory IX, Vol. 2* (Nashville, TN, 1998). Vanderbilt Univ. Press, Nashville, TN. *Innov. Appl. Math.*, pp. 205–212.
- Misiurewicz, M., 1986. Rotation intervals for a class of maps of the real line into itself. *Ergodic Theory Dynam. Systems* 6, 117–132. URL: <https://dx.doi.org/10.1017/S0143385700003321>, doi:10.1017/S0143385700003321.
- Misiurewicz, M., 2007. Rotation theory. *Scholarpedia* 2, 3873. URL: <http://www.math.iupui.edu/~mmisiure/rotth.pdf>, doi:10.4249/scholarpedia.3873.
- Moision, B.E., Orlitsky, A., Siegel, P.H., 2001. On codes that avoid specified differences. *IEEE Trans. Inform. Theory* 47, 433–442. URL: <https://ieeexplore.ieee.org/document/904557>, doi:10.1109/18.904557.
- Rota, G.C., Strang, G., 1960. A note on the joint spectral radius. *Koninklijke Nederlandse Akademie van Wetenschappen. Indagationes Mathematicae* 22, 379–381. URL: <https://www.sciencedirect.com/science/article/pii/S1385725860500461>, doi:10.1016/S1385-7258(60)50046-1.
- Shorten, R., Wirth, F., Mason, O., Wulff, K., King, C., 2007. Stability criteria for switched and hybrid systems. *SIAM Rev.* 49, 545–592. URL: https://epubs.siam.org/sirev/resource/1/siread/v49/i4/p545_s1, doi:10.1137/05063516X.
- Suzuki, H., Ito, S., Aihara, K., 2005. Double rotations. *Discrete Contin. Dyn. Syst.* 13, 515–532. URL: <http://www.aims sciences.org/article/doi/10.3934/dcds.2005.13.515>, doi:10.3934/dcds.2005.13.515.
- Tsitsiklis, J.N., Blondel, V.D., 1997. The Lyapunov exponent and joint spectral radius of pairs of matrices are hard — when not impossible — to compute and to approximate. *Math. Control Signals Systems* 10, 31–40. URL: <https://link.springer.com/article/10.1007/BF01219774>, doi:10.1007/BF01219774.
- Wirth, F., 2002. The generalized spectral radius and extremal norms. *Linear Algebra Appl.* 342, 17–40. URL: <https://www.sciencedirect.com/science/article/pii/S0024379501004463>, doi:10.1016/S0024-3795(01)00446-3.
- Wu, Z., He, Q., 2020. Optimal switching sequence for switched linear systems. *SIAM J. Control Optim.* 58, 1183–1206. URL: <https://epubs.siam.org/doi/10.1137/18M1197928>, doi:10.1137/18M1197928.

APPENDIX A. PROGRAM FOR CALCULATING THE BARABANOV NORM

The code below is written in the Python programming language versions 3.8–3.10 of the Miniconda3 (Anaconda3) distribution. This and some other related scripts for calculating the Barabanov norm can be downloaded from the website <https://github.com/kozyakin/barnorm>.

```

1  # -*- coding: utf-8 -*-
2  """Barabanov norms for rotation matrices.
3
4  Created on Sat Sep 21 12:37:46 2019.
5  Last updated on Wed Apr 27 17:07:05 2022 +0300
6
7  @author: Victor Kozyakin
8  """
9  import time
10 import math
11 from matplotlib import pyplot
12 from matplotlib.ticker import MultipleLocator
13 import numpy as np
14 import shapely
15 from shapely.geometry import LineString
16 from shapely.geometry import MultiPoint
17
18
19 def polygonal_norm(_x, _y, _h):
20     """Calculate the norm specified by a polygonal unit ball.
21
22     Args:
23         _x (real): x-coordinate of vector
24         _y (real): y-coordinate of vector
25         _h (MultiPoint): polygonal norm unit ball
26
27     Returns:
28         real: vector's norm
29     """
30     _hb = _h.boundary
31     _scale = 0.5 * math.sqrt((( _hb[2] - _hb[0])**2 + ( _hb[3] - _hb[1])**2) /
32                             (_x**2 + _y**2))
33     _l1 = LineString([(0, 0), (_scale*_x, _scale*_y)])
34     _h_int = _l1.intersection(_h).coords
35     return math.sqrt((_x**2 + _y**2) / (_h_int[1][0]**2 + _h_int[1][1]**2))
36
37
38 def min_max_norms_quotient(_g, _h):
39     """Calculate the min/max of the quotient g-norm/h-norm.
40
41     Args:
42         _g (MultiPoint): polygonal norm unit ball
43         _h (MultiPoint): polygonal norm unit ball
44
45     Returns:
46         2x0-array: minimum and maximum of g-norm/h-norm
47     """
48     _pg = _g.boundary.coords
49     _dimg = len(_pg) - 1
50     _sg = [1 / polygonal_norm(_pg[i][0], _pg[i][1], _h) for i in range(_dimg)]
51     _ph = _h.boundary.coords
52     _dimh = len(_ph) - 1

```

```

53     _sh = [polygonal_norm(_ph[i][0], _ph[i][1], _g) for i in range(_dimh)]
54     _sgh = _sg + _sh
55     return (min(_sgh), max(_sgh))
56
57
58 def matrix_angular_coord(_a, _t):
59     """Calculate the angular coordinate of vector Ax given vector x.
60
61     Args:
62         _a (2x2 np.array): input matrix A
63         _t (nx1 np.array): array of input angles of x's
64
65     Returns:
66         [nx1 np.array]: array of output angles of Ax's
67     """
68     _cos_t = math.cos(_t)
69     _sin_t = math.sin(_t)
70     _vec_t = np.asarray([_cos_t, _sin_t])
71     _vec_t_transpose = np.transpose(_vec_t)
72     _rot_back = np.asarray([[_cos_t, _sin_t], [-_sin_t, _cos_t]])
73     _vec_a = np.matmul(np.matmul(_rot_back, _a), _vec_t_transpose)
74     return _t + math.atan2(_vec_a[1], _vec_a[0])
75
76
77 # Initialization
78
79 t_tick = time.time()
80 T_BARNORM_COMP = 0.
81
82 TOL = 0.0000001
83 ANGLE_STEP = 0.01
84 LEN_TRAJECTORY = 10000
85 NUM_SYMB = 50
86 L_BOUND = 0.2
87 U_BOUND = 2.2
88
89 THETA0 = 0.7 # 0.4 # 0.6151 # one point of discontinuity
90 THETA1 = 0.8
91 COS_A0 = math.cos(THETA0)
92 SIN_A0 = math.sin(THETA0)
93 COS_A1 = math.cos(THETA1)
94 SIN_A1 = math.sin(THETA1)
95 LAMBDA = 0.75
96
97 A0 = np.asarray([[COS_A0, -SIN_A0], [SIN_A0, COS_A0]])
98 A1 = np.asarray([[COS_A1, -LAMBDA * SIN_A1], [(1 / LAMBDA) * SIN_A1, COS_A1]])
99 A0T = np.transpose(A0)
100 A1T = np.transpose(A1)
101
102 # Computation initialization
103
104 if ((np.linalg.det(A0) == 0) or (np.linalg.det(A1) == 0)):
105     raise SystemExit("Set of matrices is degenerate. End of work!")
106
107 INV_A0 = np.linalg.inv(A0)
108 INV_A1 = np.linalg.inv(A1)
109 INV_A0T = np.transpose(INV_A0)
110 INV_A1T = np.transpose(INV_A1)

```

```

111
112 p0 = np.asarray([[1, -1], [1, 1]])
113 p0 = np.concatenate((p0, -p0), axis=0)
114 p0 = MultiPoint(p0)
115 h0 = p0.convex_hull
116
117 scale0 = 1 / max(h0.bounds[2], h0.bounds[3])
118 h0 = shapely.affinity.scale(h0, xfact=scale0, yfact=scale0)
119
120 t_ini = time.time() - t_tick
121
122 print('\n #      rho_min      rho      rho_max  Num_edges\n')
123
124 # Computation iterations
125
126 NITER = 0.
127 while True:
128     t_tick = time.time()
129
130     p0 = np.asarray(MultiPoint(h0.boundary.coords))
131
132     p1 = MultiPoint(np.matmul(p0, INV_A0T))
133     h1 = p1.convex_hull
134
135     p2 = MultiPoint(np.matmul(p0, INV_A1T))
136     h2 = p2.convex_hull
137
138     h12 = h1.intersection(h2)
139     p12 = MultiPoint(h12.boundary.coords)
140
141     rho_minmax = min_max_norms_quotient(h12, h0)
142     rho_max = rho_minmax[1]
143     rho_min = rho_minmax[0]
144
145     rho = (rho_max + rho_min) / 2
146
147     h0 = h0.intersection(shapely.affinity.scale(h12, xfact=rho, yfact=rho))
148
149     T_BARNORM_COMP += (time.time() - t_tick)
150
151     NITER += 1
152     print(f'{NITER:3.0f}.', f'{rho_min:.6f}', f'{rho:.6f}', f'{rho_max:.6f}',
153           ' ', len(h0.boundary.coords) - 1)
154     scale0 = 1 / max(h0.bounds[2], h0.bounds[3])
155     h0 = shapely.affinity.scale(h0, xfact=scale0, yfact=scale0)
156
157     if (rho_max - rho_min) < TOL:
158         break
159
160 # Plotting Barabanov norm
161
162 t_tick = time.time()
163
164 h10 = shapely.affinity.scale(h1, xfact=rho, yfact=rho)
165 p10 = np.asarray(MultiPoint(h10.boundary.coords))
166
167 h20 = shapely.affinity.scale(h2, xfact=rho, yfact=rho)
168 p20 = np.asarray(MultiPoint(h20.boundary.coords))

```

```

169
170 bb = 1.7 * max(h0.bounds[2], h10.bounds[2], h20.bounds[2],
171               h0.bounds[3], h10.bounds[3], h20.bounds[3])
172
173 pyplot.rc('text', usetex=True)
174 pyplot.rc('font', family='serif')
175
176 # =====
177 # Tuning the LaTeX preamble (e.g. for international support)
178 #
179 # pyplot.rcParams['text.latex.preamble'] = \
180 #     r'\usepackage[utf8]{inputenc}' + '\n' + \
181 #     r'\usepackage[russian]{babel}' + '\n' + \
182 #     r'\usepackage{amsmath}'
183 # =====
184
185 # Plotting Barabanov's norm
186
187 fig1 = pyplot.figure(1, dpi=108)
188 ax1 = fig1.add_subplot(111)
189 ax1.set_xlim(-1.1*bb, 1.1*bb)
190 ax1.set_ylim(-1.1*bb, 1.1*bb)
191 ax1.set_aspect(1)
192 ax1.tick_params(labelsize=16)
193 ax1.grid(True, linestyle=":")
194 ax1.xaxis.set_major_locator(MultipleLocator(1))
195 ax1.yaxis.set_major_locator(MultipleLocator(1))
196
197 ax1.plot(p10[:, 0], p10[:, 1], ':', color='red', linewidth=1.25)
198 ax1.plot(p20[:, 0], p20[:, 1], '--', color='blue', linewidth=1)
199 ax1.plot(p0[:, 0], p0[:, 1], '-.', color='black')
200
201 # Plotting lines of intersection of norms' unit spheres
202
203 pl10 = LineString(p10)
204 pl20 = LineString(p20)
205 h_int = np.asarray(shapely.affinity.scale(pl10.intersection(pl20),
206                                           xfact=3, yfact=3))
207 arr_switch_N = np.size(h_int[:, 0])
208 arr_switch_ang = np.empty(arr_switch_N)
209 for i in range(np.size(h_int[:, 0])):
210     arr_switch_ang[i] = math.atan2(h_int[i, 1], h_int[i, 0])
211     if arr_switch_ang[i] < 0:
212         arr_switch_ang[i] = arr_switch_ang[i] + 2. * math.pi
213     if h_int[i, 0] >= 0:
214         ax1.plot([2 * h_int[i, 0], -2 * h_int[i, 0]],
215                 [2 * h_int[i, 1], -2 * h_int[i, 1]],
216                 dashes=[5, 2, 1, 2], color='green', linewidth=1)
217
218 t_plot_fig1 = time.time() - t_tick
219 pyplot.show()
220
221
222 # Plotting an extremal trajectory
223
224 t_tick = time.time()
225
226 fig2 = pyplot.figure(1, dpi=108)

```

```

227 ax2 = fig2.add_subplot(111)
228 ax2.set_xlim(-1.1*bb, 1.1*bb)
229 ax2.set_ylim(-1.1*bb, 1.1*bb)
230 ax2.set_aspect(1)
231 ax2.tick_params(labelsize=16)
232 ax2.grid(True, linestyle=":")
233 ax2.xaxis.set_major_locator(MultipleLocator(1))
234 ax2.yaxis.set_major_locator(MultipleLocator(1))
235
236 # Plotting lines of intersection of norms' unit spheres
237
238 arr_switch_N = np.size(h_int[:, 0])
239 arr_switch_ang = np.empty(arr_switch_N)
240 for i in range(np.size(h_int[:, 0])):
241     arr_switch_ang[i] = math.atan2(h_int[i, 1], h_int[i, 0])
242     if arr_switch_ang[i] < 0:
243         arr_switch_ang[i] = arr_switch_ang[i] + 2. * math.pi
244     if h_int[i, 0] >= 0:
245         ax2.plot([2 * h_int[i, 0], -2 * h_int[i, 0]],
246                 [2 * h_int[i, 1], -2 * h_int[i, 1]],
247                 dashes=[5, 2, 1, 2], color='green', linewidth=1)
248
249
250 # Plotting the trajectory
251
252 x = np.asarray([1, 1])
253
254 if rho > 1:
255     x = (L_BOUND / polygonal_norm(x[0], x[1], h0)) * x
256 else:
257     x = (U_BOUND / polygonal_norm(x[0], x[1], h0)) * x
258
259 for i in range(LEN_TRAJECTORY):
260     xprev = x
261     x0 = np.matmul(x, A0T)
262     x1 = np.matmul(x, A1T)
263     if (polygonal_norm(x0[0], x0[1], h0) >
264         polygonal_norm(x1[0], x1[1], h0)):
265         x = x0
266         ax2.arrow(xprev[0], xprev[1], x[0]-xprev[0], x[1]-xprev[1],
267                 head_width=0.04, head_length=0.08, linewidth=0.75,
268                 color='red', length_includes_head=True, zorder=-i)
269     else:
270         x = x1
271         ax2.arrow(xprev[0], xprev[1], x[0]-xprev[0], x[1]-xprev[1],
272                 head_width=0.04, head_length=0.08, linewidth=0.75,
273                 color='blue', length_includes_head=True, zorder=-i)
274     if ((polygonal_norm(x[0], x[1], h0) > U_BOUND) or
275         (polygonal_norm(x[0], x[1], h0) < L_BOUND)):
276         break
277
278 arr_switch_ang.sort()
279 ISPLIT = 0
280 for i in range(np.size(arr_switch_ang)):
281     if arr_switch_ang[i] < math.pi:
282         ISPLIT = i
283
284 arr_switch_ang = np.resize(arr_switch_ang, ISPLIT + 1)

```

```

285 arr_switch_N = np.size(arr_switch_ang)
286 arr_switches = np.insert(arr_switch_ang, 0, 0)
287 arr_switches = np.append(arr_switches, math.pi)
288 omega1 = (arr_switches[1] + arr_switches[2])/2.
289 omega2 = omega1 + math.pi/2.
290 omega3 = omega2 + math.pi/2.
291 omega4 = omega3 + math.pi/2.
292 props = dict(boxstyle='round', facecolor='gainsboro', edgecolor='none',
293             alpha=0.5)
294 p_label = np.array([math.cos(omega1), math.sin(omega1)])
295
296 if (polygonal_norm(p_label[0], p_label[1], h10) >
297     polygonal_norm(p_label[0], p_label[1], h20)):
298     ax2.text(0.9 * bb * math.cos(omega1), 0.9 * bb * math.sin(omega1),
299             r'$x_{n+1}=A_0x_n$', ha='center', va='center',
300             fontsize='x-large', bbox=props)
301     ax2.text(0.8 * bb * math.cos(omega2), 0.8 * bb * math.sin(omega2),
302             r'$x_{n+1}=A_1x_n$', ha='center', va='center',
303             fontsize='x-large', bbox=props)
304     ax2.text(0.9 * bb * math.cos(omega3), 0.9 * bb * math.sin(omega3),
305             r'$x_{n+1}=A_0x_n$', ha='center', va='center',
306             fontsize='x-large', bbox=props)
307     ax2.text(0.8 * bb * math.cos(omega4), 0.8 * bb * math.sin(omega4),
308             r'$x_{n+1}=A_1x_n$', ha='center', va='center',
309             fontsize='x-large', bbox=props)
310 else:
311     ax2.text(0.8 * bb * math.cos(omega1), 0.8 * bb * math.sin(omega1),
312             r'$x_{n+1}=A_1x_n$', ha='center', va='center',
313             fontsize='x-large', bbox=props)
314     ax2.text(0.9 * bb * math.cos(omega2), 0.9 * bb * math.sin(omega2),
315             r'$x_{n+1}=A_0x_n$', ha='center', va='center',
316             fontsize='x-large', bbox=props)
317     ax2.text(0.8 * bb * math.cos(omega3), 0.8 * bb * math.sin(omega3),
318             r'$x_{n+1}=A_1x_n$', ha='center', va='center',
319             fontsize='x-large', bbox=props)
320     ax2.text(0.9 * bb * math.cos(omega4), 0.9 * bb * math.sin(omega4),
321             r'$x_{n+1}=A_0x_n$', ha='center', va='center',
322             fontsize='x-large', bbox=props)
323
324 t_plot_fig2 = time.time() - t_tick
325 pyplot.show()
326
327 # Plotting the angular functions
328
329 t_tick = time.time()
330
331 fig3 = pyplot.figure(2, dpi=108)
332 ax3 = fig3.add_subplot(111)
333 ax3.set_xlim(0., math.pi)
334 ax3.set_ylim(0., math.pi)
335 ax3.set_aspect(1)
336 ax3.tick_params(labelsize=16)
337
338 t = np.arange(0., math.pi, ANGLE_STEP)
339 angle_arr_A0 = np.empty(len(t))
340 angle_arr_A1 = np.empty(len(t))
341 for i, item in enumerate(t):
342     angle_arr_A0[i] = matrix_angular_coord(A0, item)

```

```

343     angle_arr_A1[i] = matrix_angular_coord(A1, item)
344
345 ax3.plot(t, angle_arr_A0, linestyle=(0, (30, 30)), color='red',
346         linewidth=0.15)
347 ax3.plot(t, angle_arr_A0 + math.pi, linestyle=(0, (30, 30)), color='red',
348         linewidth=0.15)
349 ax3.plot(t, angle_arr_A0 - math.pi, linestyle=(0, (30, 30)), color='red',
350         linewidth=0.15)
351 ax3.plot(t, angle_arr_A1, linestyle=(0, (30, 30)), color='blue',
352         linewidth=0.15)
353 ax3.plot(t, angle_arr_A1 + math.pi, linestyle=(0, (30, 30)), color='blue',
354         linewidth=0.15)
355 ax3.plot(t, angle_arr_A1 - math.pi, linestyle=(0, (30, 30)), color='blue',
356         linewidth=0.15)
357
358 # Plotting the angular function delivering
359 # the maximal growth rate of iterations
360
361 for j in range(arr_switch_N + 1):
362     t = np.arange(arr_switches[j], arr_switches[j + 1], ANGLE_STEP)
363     angle_arr_A0 = np.empty(len(t))
364     angle_arr_A1 = np.empty(len(t))
365     for i, item in enumerate(t):
366         angle_arr_A0[i] = matrix_angular_coord(A0, item)
367         angle_arr_A1[i] = matrix_angular_coord(A1, item)
368     omega = (arr_switches[j] + arr_switches[j + 1]) / 2.
369     x = np.asarray([math.cos(omega), math.sin(omega)])
370     x0 = np.matmul(x, A0T)
371     x1 = np.matmul(x, A1T)
372     if (polygonal_norm(x0[0], x0[1], h0) <
373         polygonal_norm(x1[0], x1[1], h0)):
374         ax3.plot(t, angle_arr_A1, 'b', linewidth=1.5)
375         ax3.plot(t, angle_arr_A1 + math.pi, 'b', linewidth=1.5)
376         ax3.plot(t, angle_arr_A1 - math.pi, 'b', linewidth=1.5)
377     else:
378         ax3.plot(t, angle_arr_A0, 'r', linewidth=1.5)
379         ax3.plot(t, angle_arr_A0 + math.pi, 'r', linewidth=1.5)
380         ax3.plot(t, angle_arr_A0 - math.pi, 'r', linewidth=1.5)
381
382 # Putting Pi-ticks on axes
383
384 xtick_pos = [0, arr_switches[1], 0.5 * np.pi, arr_switches[2], np.pi]
385 xlabels = [r'0', r'$\omega_0$', '', r'$\omega_1$', r'$\pi$']
386 ytick_pos = [0, 0.5 * np.pi, np.pi]
387 ylabels = [r'0', r'$\frac{\pi}{2}$', r'$\pi$']
388
389 pyplot.xticks(xtick_pos, xlabels)
390 pyplot.yticks(ytick_pos, ylabels)
391 pyplot.grid(linestyle=":")
392
393 t_plot_fig3 = time.time() - t_tick
394 pyplot.show()
395
396 # Calculating index sequence
397
398 t_tick = time.time()
399
400 F0 = 0.

```

```

401 F1 = 0.
402 F00 = 0.
403 F01 = 0.
404 F10 = 0.
405 F11 = 0.
406 x = np.asarray([1, 1])
407 index_seq = []
408
409 for i in range(LEN_TRAJECTORY):
410     x = x / polygonal_norm(x[0], x[1], h0)
411     x0 = np.matmul(x, A0T)
412     x1 = np.matmul(x, A1T)
413     if (polygonal_norm(x0[0], x0[1], h0) >
414         polygonal_norm(x1[0], x1[1], h0)):
415         x = x0
416         index_seq.append('0')
417         F0 += 1
418     else:
419         x = x1
420         index_seq.append('1')
421         F1 += 1
422     if i > 0:
423         if ((index_seq[i-1] == '0') and (index_seq[i] == '0')):
424             F00 += 1
425         if ((index_seq[i-1] == '0') and (index_seq[i] == '1')):
426             F01 += 1
427         if ((index_seq[i-1] == '1') and (index_seq[i] == '0')):
428             F10 += 1
429         if ((index_seq[i-1] == '1') and (index_seq[i] == '1')):
430             F11 += 1
431
432 print('\nExtremal index sequence: ', end='')
433 for i in range(NUM_SYMB):
434     print(index_seq[i], end='')
435
436 print('\n\nFrequencies of symbols 0, 1, 00, 01 etc. in the index sequence:',
437       '\n\nSymbols:      0      1      00      01      10      11')
438
439 print('Frequencies: ',
440       f' {round(F0/LEN_TRAJECTORY, 3):.3f}',
441       f' {round(F1/LEN_TRAJECTORY, 3):.3f}',
442       f' {round(F00/(LEN_TRAJECTORY-1), 3):.3f}',
443       f' {round(F01/(LEN_TRAJECTORY-1), 3):.3f}',
444       f' {round(F10/(LEN_TRAJECTORY-1), 3):.3f}',
445       f' {round(F11/(LEN_TRAJECTORY-1), 3):.3f}')
446
447 t_index_seq = time.time() - t_tick
448
449 # Saving plots to pdf-files
450
451 """
452 fig1.savefig(f'bnorm-{THETA0:.2f}-{THETA1:.2f}-{LAMBDA:.2f}.pdf',
453             bbox_inches='tight')
454 fig2.savefig(f'etraj-{THETA0:.2f}-{THETA1:.2f}-{LAMBDA:.2f}.pdf',
455             bbox_inches='tight')
456 fig3.savefig(f'sfunc-{THETA0:.2f}-{THETA1:.2f}-{LAMBDA:.2f}.pdf',
457             bbox_inches='tight')
458 """

```



```

459
460 # Computation timing
461
462 t_compute = T_BARNORM_COMP + t_index_seq
463 t_total = (t_ini + t_plot_fig3 + t_plot_fig2 + t_plot_fig1 + t_compute)
464 t_plot = (t_plot_fig1 + t_plot_fig2 + t_plot_fig3)
465
466 print('\nInitialization: ', f'{round(t_ini, 6):6.2f} sec.')
467 print('Computations:      ', f'{round(t_compute, 6):6.2f} sec.')
468 print('Plotting:           ', f'{round(t_plot, 6):6.2f} sec.')
469 print('Total:              ', f'{round(t_total, 6):6.2f} sec.')

```

LISTING 1. Python code `barnorm_rot.py` for computing the Barabanov norm of a pair of matrices and the angular function of the iterations at which the joint spectral radius is reached

INSTITUTE FOR INFORMATION TRANSMISSION PROBLEMS, RUSSIAN ACADEMY OF SCIENCES, BOLSHOJ KARETNY
 LANE 19, MOSCOW 127051, RUSSIA
Email address: `kozyakin@iitp.ru`